DIABETES TECHNOLOGY & THERAPEUTICS
Volume 5, Number 5, 2003

Military Metabolic Monitoring

Systemic Effects of Shock and Resuscitation Monitored by Visible Hyperspectral Imaging

ROBERT GILLIES, Ph.D.,[1] JENNY E. FREEMAN, M.D., F.A.C.S.,[1]
LEOPOLDO C. CANCIO, M.D., F.A.C.S., LTC, MC, U.S.Army,[2] DEREK BRAND, B.Sc.,[1]
MICHAEL HOPMEIER, M.S.M.E.,[1] and JAMES R. MANSFIELD, M.Sc.[1]

ABSTRACT

Hyperspectral imaging (HSI) has been useful in monitoring several medical conditions, which to date have generally involved local changes in skin oxygenation of isolated regions of interest such as skin flaps or small burns. Here, by contrast, we present a study in which HSI was used to assess the local cutaneous manifestations of significant systemic events. HSI of the ventral surface of the lower jaw was used to monitor changes in skin oxygenation during hypovolemic shock induced by hemorrhage with additional pulmonary contusion injury in a porcine model, and to monitor the subsequent recovery of oxygenation with resuscitation. Quantitative and qualitative changes were observed in the level of skin oxygenation during shock and recovery. Quantitative values were obtained by fitting reference spectra of oxyhemoglobin and deoxyhemoglobin to sample spectra. Qualitative changes included changes in the observed spatial distribution or pattern of skin oxygenation. A mottled pattern of oxygen saturation was observed during hemorrhagic shock, but not observed during hypovolemic shock or following resuscitation. Historically, the assessment of skin color and mottling has been an important, albeit inexact, component of resuscitation algorithms. Now, it is possible to analyze these variables during shock and resuscitation in an objective manner. The clinical utility of these advances needs to be determined.

INTRODUCTION

THERE IS A GLOBAL NEED for improved methods of metabolic monitoring. Among these different applications are: healthy athlete-soldiers during physical exertion; astronauts during extravehicular activity; brittle diabetics experiencing diurnal and sporadic fluctuations in insulin and glucose levels; and injured patients with hemorrhagic shock. Chronic metabolic aberrations such as diabetes could also benefit from methodologies targeting the effectiveness of physiologic control. To be maximally useful, metabolic monitoring should be non-invasive and easy to use.

Hyperspectral (HS) imaging (HSI), in one

[1]HyperMed, Inc., Watertown, Massachusetts.
[2]U.S. Army Institute of Surgical Research, Ft. Sam Houston, Texas.
This work was presented in part at SPIE Photonics West 2000, held in San Jose, California.

Report Documentation Page

Form Approved
OMB No. 0704-0188

1. REPORT DATE	2. REPORT TYPE	3. DATES COVERED
05 JUL 2004	**N/A**	**-**

4. TITLE AND SUBTITLE	5a. CONTRACT NUMBER
Systemic effects of shock and resuscitation monitored by visible hyperspectral imaging	5b. GRANT NUMBER
	5c. PROGRAM ELEMENT NUMBER
6. AUTHOR(S)	5d. PROJECT NUMBER
Gillies R., Freeman J. E., Cancio L. C., Brand D., Hopmeier M., Mansfield J. R.,	5e. TASK NUMBER
	5f. WORK UNIT NUMBER
7. PERFORMING ORGANIZATION NAME(S) AND ADDRESS(ES)	8. PERFORMING ORGANIZATION REPORT NUMBER
United States Army Institute of Surgical Research, JBSA Fort Sam Houston, TX 78009	
9. SPONSORING/MONITORING AGENCY NAME(S) AND ADDRESS(ES)	10. SPONSOR/MONITOR'S ACRONYM(S)
	11. SPONSOR/MONITOR'S REPORT NUMBER(S)

12. DISTRIBUTION/AVAILABILITY STATEMENT
Approved for public release, distribution unlimited

13. SUPPLEMENTARY NOTES

14. ABSTRACT

15. SUBJECT TERMS

16. SECURITY CLASSIFICATION OF:			17. LIMITATION OF ABSTRACT	18. NUMBER OF PAGES	19a. NAME OF RESPONSIBLE PERSON
a. REPORT	b. ABSTRACT	c. THIS PAGE			
unclassified	**unclassified**	**unclassified**	**SAR**	**9**	

guise or another, has become a useful tool for the investigation of spatial heterogeneity in spectral properties in a variety of fields of study ranging from astronomy to medicine. Originally developed by the Department of Defense (DoD) for military purposes, HSI has been used for decades in airplane- and satellite-mounted systems for the mapping of land use and soil types; it has moved in the last 5 years into a large number of application areas.[1,2] Of particular interest here is the use of HSI in the fields of biophysics and medicine. The combination of spectroscopic imaging and microscopy has proved very useful in the investigation of the spectral properties of slices of tissue.[3,4] In addition to being useful for the investigation of microscopic structures, HSI systems for imaging macroscopic structures have been shown to be useful in the monitoring of the spatial distribution of skin oxygenation.[5,6]

Spectroscopic methods have been used for over 2 decades to monitor oxygen levels in a variety of tissues in operating theatres in the form of pulse oximeters.[7] These simple systems utilize the different oxy- and deoxyhemoglobin absorption bands to determine arterial oxygen saturation. However, one of the drawbacks of fiber optic-based commercial systems for monitoring tissue oxygenation is that they sample only one region or volume of tissue and give us no information about the spatial distribution of the reading. HSI, however, allows mapping of the regional variations in hemodynamic parameters in response to tissue perfusion. Unlike infrared thermography, this approach does not map the thermal emission of the tissues. Instead, HSI relies on the differential absorption of light by oxy- and deoxyhemoglobin, resulting in differences in the wavelength dependence of the tissue reflectance depending on the hemoglobin oxygen saturation (O_2sat) of that tissue. Changes in the absolute amounts of hemoglobin can be difficult to determine quantitatively; however, determining the relative amounts of hemoglobin O_2sat is relatively easy given the differing spectra of these two moieties.

One application of HSI has been in the determination of tissue viability following plastic surgery. Tissue that has insufficient oxygenation to remain viable is readily apparent from O_2sat maps calculated from near-infrared or visible spectral images acquired immediately following surgery; clinical signs of the loss of viability do not become apparent for 6–12 h post-surgery.[8,9] Assessments of tissue viability following partial thickness skin burns using HSI have also been done.[10,11]

However, HSI has not been previously applied to systemic conditions such as shock. Shock is a clinical syndrome in which there is inadequate perfusion to, and therefore oxygenation of, end organs. Its causes include hemorrhage, cardiac failure, sepsis, hypoglycemia, and burns; the pathophysiology of these various shock states is quite different. Depending on the cause of shock, the skin is one organ that readily manifests its effects. The importance of skin oxygenation is well known to the clinician and recognized in resuscitation programs such as Pediatric Advanced Life Support: "Decreased perfusion of the skin can be an early sign of shock . . . Mottling, pallor, delayed capillary refill, and peripheral cyanosis often indicate poor skin perfusion."[12] Nevertheless, resuscitation of patients with shock is typically directed toward restoring quantifiable systemic variables (e.g., pulse, blood pressure, cardiac output).

Systemic hemodynamic data, however, may fail to detect inadequate correction of end-organ perfusion. Also, the devices used to obtain these data are usually placed invasively. Thus, their placement is often time-consuming—which may delay the treatment of critically ill patients—and is associated with the risk of side effects. Despite the shortcomings of these systemic variables, data that reflect end-organ perfusion (e.g., urine output) are rarely available in real time. Only a few current technologies provide real-time end-organ perfusion data, and these have not been widely implemented.

HSI technology can be developed into a robust end-user device for the field or clinic. HSI offers the possibility to monitor physiologic states, which can be studied by quantifying and depicting spatial changes in hemoglobin O_2sat in the skin. Relating these local changes to systemic physiology will provide a generic understanding of the capabilities and limitations of HSI, and permit it to be generalized to other areas in which non-invasive metabolic monitoring would be highly advantageous.

Accordingly, this study evaluated the ability of a HSI system to depict and quantify the cutaneous manifestations of shock in an effort to develop a new, non-invasive method for monitoring shock patients. A porcine model was used, in which shock was induced by chest trauma followed by hemorrhage.

MATERIALS AND METHODS

Operative procedures

This study was conducted as an addendum to an existing protocol in an Association for Assessment and Accreditation of Laboratory Animal Care-approved facility, in accordance with applicable National Institutes of Health (NIH) and DoD regulations on the care of laboratory animals. A single 30-kg female swine was anesthetized throughout the experiment with intravenous ketamine and propofol by continuous infusion. Depth of anesthesia was verified before all painful procedures, and was monitored by means of a bispectral EEG (Aspect Medical Systems, Inc.). In the operating room, a tracheostomy was performed, and the external jugular vein, pulmonary artery, femoral artery, and femoral vein were catheterized. The animal was transferred to an animal intensive care unit and was mechanically ventilated (Servo 900, Siemens). The following data were continuously acquired to a computerized system: systemic arterial, central venous, and pulmonary arterial pressures; thermodilution cardiac output; mixed venous and pulse oximetric O_2sat; end-tidal carbon dioxide tension; and blood temperature.

After baseline studies and nebulization with normal saline, a captive-bolt humane stunner (Karl Schermer), modified by attachment of a 7.5-cm-diameter plate to the bolt, was used to cause a blunt right chest injury. A tube thoracostomy was immediately performed. After a 10-min period, during which the vital signs partially recovered, the animal underwent a constant-volume, fixed-rate hemorrhage of 12 mL/kg over a 12-min period. A 30-min shock period ensued, after which the animal was resuscitated with lactated Ringer's solution (3× shed blood volume) by rapid intravenous bolus infusion. Three hours after injury, the animal was euthanized with a standard veterinary barbiturate solution.

Image collection

At multiple time points during the experiment, HS images were obtained of the ventral surface of the submandibular area (~15 × 10 cm in total area). Fiducial marks were placed on the skin ~8 cm apart to facilitate image registration. Images were collected using a Kodak MEGAPLUS 1.6i charge coupled device (CCD) camera consisting of a 1,024 × 1,532 CCD element and a 10-bit A/D converter (Eastman Kodak Co.). Images were collected as full arrays, then binned down to 256 × 383 images. The camera was fitted with a Nikon Micro AF60 lens with the *f*-stop set to 8. Quartz halogen lamps evenly illuminated the surface of the samples. A liquid crystal tunable filter (5 nm bandpass) from Cambridge Research & Instrumentation (Woburn, MA) was placed over the camera lens to provide wavelength selection 500–600 nm at 5-nm intervals. Sample images were combined to form a sample image cube; two dimensions of the cube represented the spatial component of each image, and the third dimension represented the spectral component of the images.

A reference image cube was acquired using the white surface of a Kodak GreyCard placed carefully over the field of interest and imaged with the same parameters used to acquire the sample image cube. These images, which account for the lighting variations across the region of interest, serve as the analysis reference.

In general, the quality of the spectra collected was high. There were few motion artifacts in the data, and the lighting remained consistent throughout the data collection period.

Image analysis

Raw sample images (S) and reference images (R) were smoothed using a three-point mean filter along spectral dimension of the image cubes. The smoothed sample image cubes (S) were ratioed against the smoothed reference image cubes (R) to convert the data to an optical density scale (A). The optical density at pixel i,j (A_{ij}) of each raw image was calculated by:

$$A_{ij} = -\log_{10}(S_{ij}/R_{ij}) \quad (1)$$

The conversion of the data to optical density allowed the spectra to be analyzed using standard spectroscopic algorithms.[13] Three least squares fit coefficients, c_1, c_2, and c_3, were calculated for each spectrum in an image cube from in vivo reference spectra taken from the literature[14] (Fig. 1) for oxyhemoglobin, deoxyhemoglobin, and an offset spectrum, respectively, by:

$$\vec{S}_{ij} = \|c_1 \overrightarrow{OxyHb} + c_2 \overrightarrow{DeoxyHb} + c_3 \overrightarrow{Offset}\|_2 \quad (2)$$

These coefficients allowed the determination of the relative total hemoglobin (THb) concentration:

$$\text{THb} = THb_{ij} = c_{\text{oxy}_{ij}} + c_{\text{deoxy}_{ij}} \quad (3)$$

and relative percent O_2sat:

$$\%O_2\text{sat}_{ij} = [c_{\text{oxy}_{ij}}/(THb_{ij})] \times 100 \quad (4)$$

at each pixel location. Gray-scale images based on these values were analyzed using standard image analysis techniques.

RESULTS

A time series of percent O_2sat images are shown in Figure 2. Each image shows a 10 cm × 10 cm skin area. Although some motion artifacts are evident in several of the images (in particular the 2:00 min and 9:00 min images), these artifacts do not affect the overall spatial variations observed in skin oxygenation. The images for time points from −40 min to −25 min (pre-contusion) are shown with an expanded region of interest. The pig moved a considerable distance following contusion, and the alignment of the images in the field of view of the imaging system was not the same pre- and post-contusion.

All pre-contusion images in Figure 2 show a relatively stable and even oxygenation, with the possible exception of the −27 min image (immediately following the start of nebulization), which may show a small amount of mottling. All post-resuscitation images (57 min and on) also show a relatively even pattern of skin oxygenation. The most striking changes seen in these images were the spatial heterogeneity, or mottling, seen in the 23–47-min images. These corresponded to those time points during which the animal was in a

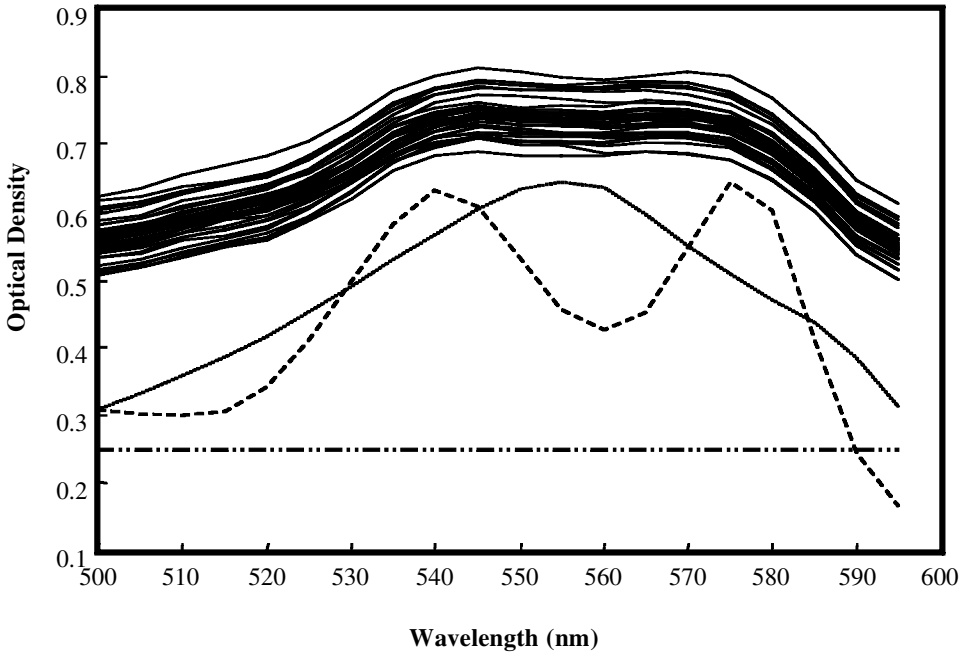

FIG. 1. Representative sample skin reflectance spectra from the central portion of the submandibular area of a pig (solid lines) and the oxyhemoglobin (dashed line), deoxyhemoglobin (dotted line), and offset (dashed-dotted line) spectra that were used for the least squares fits in Eq. 2.

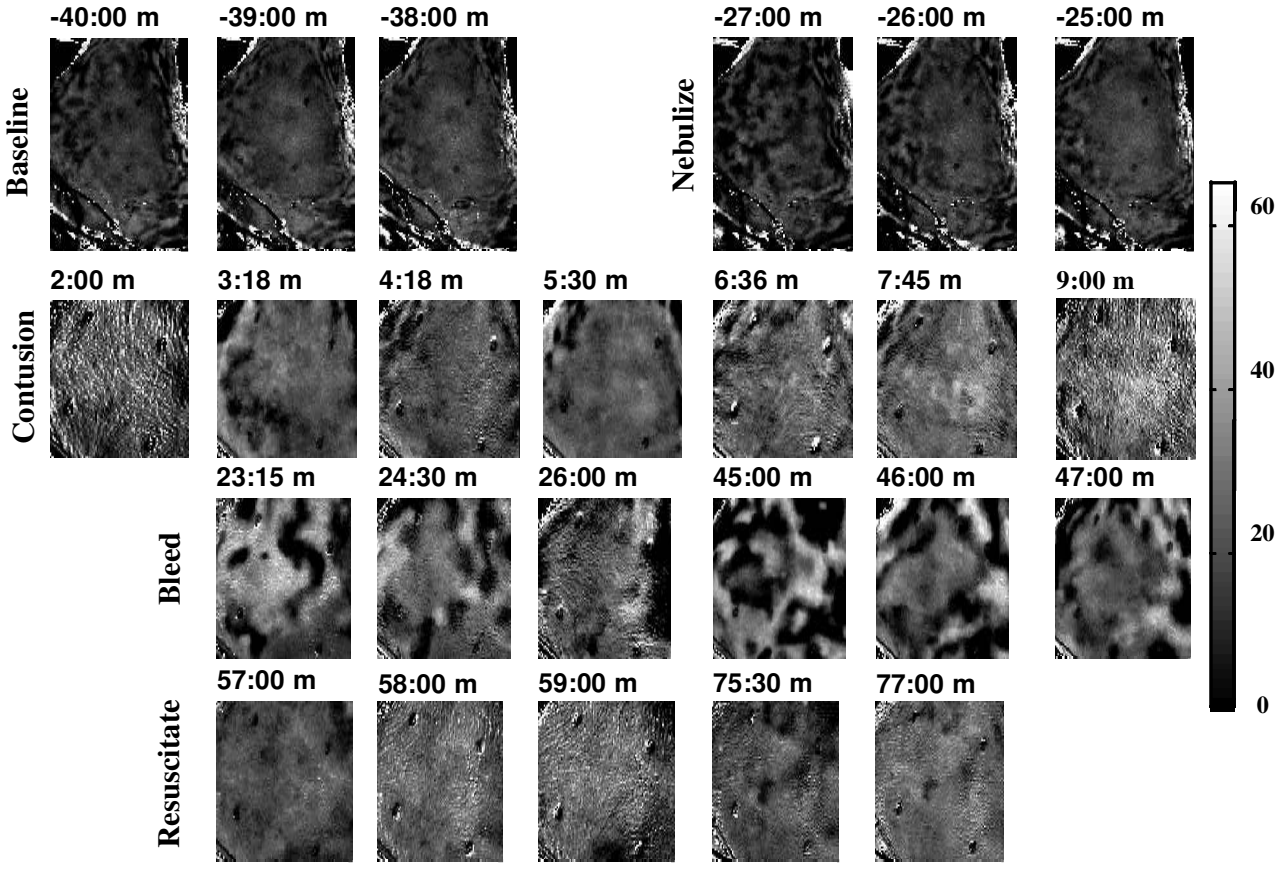

FIG. 2. O_2sat images obtained from the ventral surface of the submandibular area of the pig. The intervention is listed at the left for each series of images, and the time is at the top of each image. Trauma was induced at $t = 0$ min. Bright areas represent high oxygenation, and dark areas represent low oxygenation.

state of hemorrhagic shock. The marked increase in mottling seen in the O_2sat images during hemorrhagic shock was not readily apparent to unaided observers at the bedside. Immediately following bleeding (23 min), no visible mottling was observed. One senior clinician noted faint mottling towards the end of the shock period, but the mottling was not obvious. While the mottling pattern is clearly visible in the O_2sat images, mottling is not observed in either the THb or offset images (see Fig. 3). Although large changes in the spatial heterogeneity (mottling) in skin oxygenation during shock were observed, the average O_2sat of all of the images remained approximately constant during the entire procedure and did not vary systematically with shock ($R = 0.23$).[15]

DISCUSSION

Relative O_2sat images computed from the HSI data showed significant changes with injury, bleeding, and resuscitation, although the nature of these changes appeared to be complex. Of particular note was the increased regional variability or "mottled pattern" of skin oxygenation observed from the onset through the duration of hemorrhagic shock. A mottled appearance of the skin is often used as a clinical sign of shock. The THb and offset images, by contrast, are relatively stable and, more importantly, do now show any of the signs of mottling seen in the O_2sat images. This suggests that the changes in the spatial distribution of skin O_2sat seen during hemorrhagic shock may not be related to blood volume or to optical scattering, but simply to oxygenation changes of the hemoglobin in the skin.

The principal explanation for the mottled pattern after hemorrhagic shock is that a decrease in blood flow has occurred, increasing tissue oxygen extraction from available oxyhemoglobin and resulting in a predominance of deoxyhemoglobin in the local environment. There are

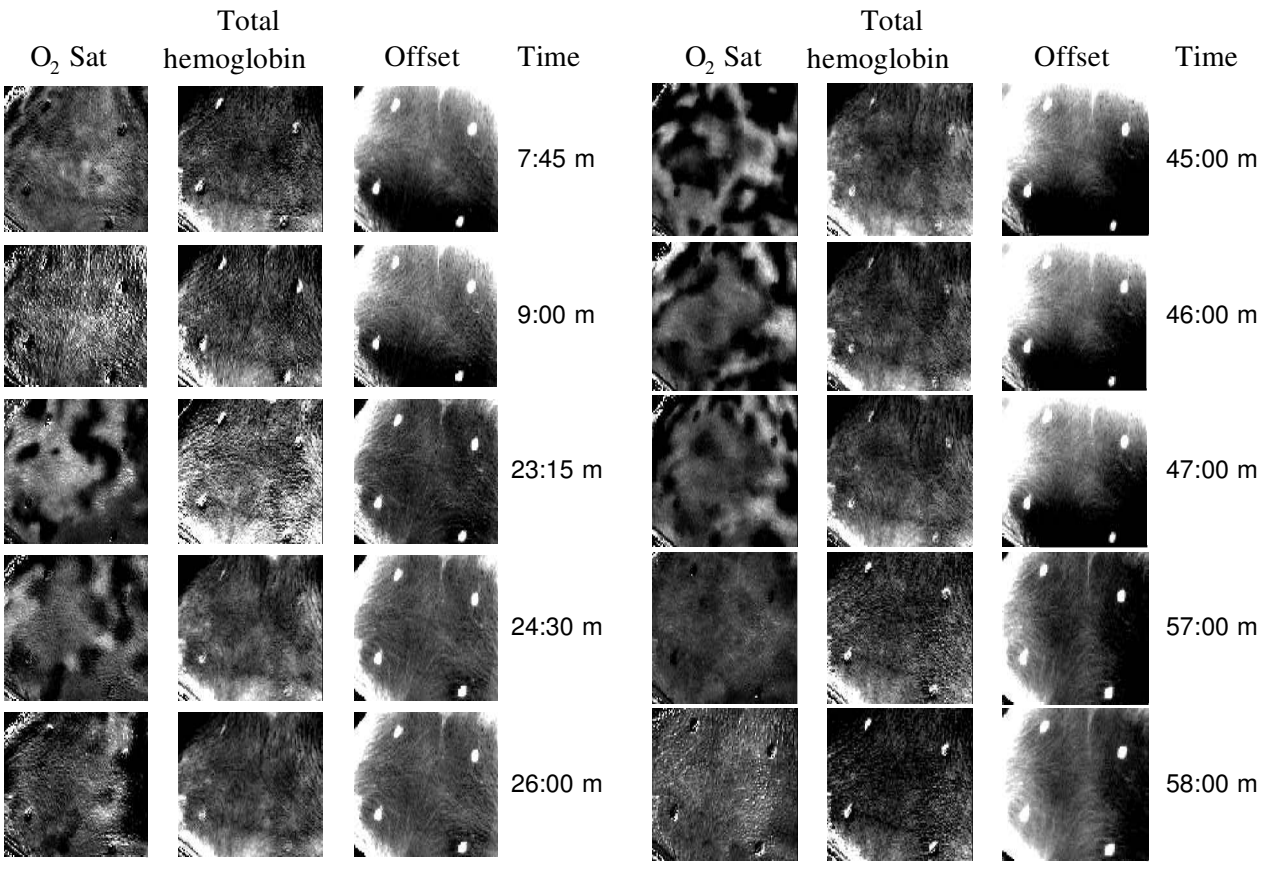

FIG. 3. O_2sat, THb, and offset images (**left to right**) obtained 7 min 45 s to 58 min after trauma was induced. Bright areas represent high oxygenation, and dark areas represent low oxygenation.

a number of factors affecting the microvasculature of the skin that could account for a decrease in blood flow under these circumstances. The arterioles and venules of the skin are innervated by fibers of the sympathetic nervous system (SNS), which orchestrates the body's response to a decrease in central blood volume. Hypovolemia induces an increase in SNS output, which, as a rule, causes cutaneous vasoconstriction. The juxtaposition of areas of high and low O_2sat during shock also suggests that the SNS centrally controlled oscillations[16–20] in blood flow through adjacent arterioles are not in phase, resulting in an increase of the amplitude of skin blood-flow oscillations.

In addition, various mediators affect the cutaneous microvasculature and could be responsible for the effects seen in these data. Epinephrine and norepinephrine, which increase in response to hemorrhagic shock, cause vasoconstriction. On the other hand, vasoactive amines such as histamine and bradykinin may be released by massive pulmonary contusion and cause vasodilation. The various prostaglandins known released by this injury cause either vasodilation or vasoconstriction.[21] Intravital microscopy has demonstrated that hemorrhagic shock causes constriction of larger arterioles (156 μm) and venules (365 μm), but not of pre- or post-capillary vessels, in a hamster dorsal skinfold model.[22] Porphyrin phosphorescence decay was used in that model to demonstrate that hemorrhagic shock causes "dissociation" of central and local pO_2: P_aO_2 increases, but arteriolar, venular, and tissue pO_2 decrease.[23,24]

Although at this time there is no means of determining the causal factor(s) in the appearance of mottling during shock, the findings above may help explain the "dark" areas in the images shown between 23 min 15 s and 47 min in Figure 3. Vasoconstriction causes decreased blood flow, which causes greater oxygen extraction by the tissue from the available hemo-

globin. The "bright" areas in the oxygenation images are more difficult to explain, but may represent arteriovenous shunting. Interestingly, the THb content of the skin did not change with the onset of hypovolemic shock. The THb levels (second and fifth columns in Fig. 3) remained relatively constant during the procedure and showed no signs of the obvious mottling seen in the O_2sat images during hypovolemic shock. This points to difference in oxygen extraction and blood flow during shock rather than changes in the amount of blood in the skin at any one time.

Post-contusion shock is poorly understood; in particular, the effects of contusion on distal cutaneous blood flow are unknown. The decrease in central venous pressure, in the absence of significant blood loss, argues in favor of peripheral vasodilation and decreased preload as a causative factor. In addition, the increase in pulmonary artery pressure immediately following trauma indicates an increase in right-heart afterload. Both phenomena are likely mediated, at least in part, by massive mediator release following injury.

Transcutaneous ($tcpO_2$) monitoring, by means of a Clark electrode applied to the skin, has been used in the neonatal intensive care unit because the $tcpO_2$ correlates with the p_aO_2 in that setting. In adults in shock, however, these values do not correlate. However, given the spatial heterogeneity seen in this study, it seems reasonable that a single-point measurement of skin oxygenation (like $tcpO_2$) would not provide optimal data to monitor shock. The changing patterns of high and low regions of oxygenation require an imaging method to monitor them.

Because HSI technology is relatively inexpensive and rugged, it is possible to make portable field or clinical HSI systems. Technology of this type has long been in use by the DoD for aerial detection and identification of hidden combat vehicles.[25] There is also considerable need for HSI in the military medicine. Frontline combat casualties present unique challenges. Weight and size determine which technologies may be used. Treatment and monitoring modalities used routinely in an intensive care unit setting are not feasible in combat. HSI may provide a noninvasive and lightweight technique to monitor soldiers experiencing extreme metabolic stress secondary to injury, and the subsequent efficacy of treatment. It is possible that noninvasive HSI methods based on hemoglobin oxygenation will become useful in monitoring various types of shock and in the triage of such patients. It is critical to be able to rapidly and noninvasively determine the shock status of wounded soldiers on a battlefield, and to be able to monitor to optimize resuscitation and minimize wasted resources.

Other applications of HSI can also capitalize on its capabilities to monitor the metabolic state of tissue. An important use of this technology that has recently been investigated is its potential use in the ongoing care of people with diabetes (J. Mansfield et al., manuscript in preparation). Diabetics are at high risk for limb loss secondary to atherosclerotic peripheral vascular disease or diabetic foot ulceration.[26] HSI may be useful in the assessment of peripheral lesions of this nature, in the early detection of infection, and/or in the monitoring of the response to therapy. Peripheral vascular disease, with its subsequent compromise in tissue perfusion, also is a potential application for HSI, which may be useful in the early detection and assessment of peripheral compromise and lesions. Monitoring spatial changes in the skin oxygenation may provide an objective measure of the extent and severity of vascular compromise. In addition to its utility in the assessment of shock, HSI may also be useful in assessing compromised perfusion in the feet of diabetics and in determining whether a given foot is at risk of developing an ulcer, or in assessing the degree of success in restoring normal perfusion to the lower limb following vascular surgery. Studies of both types are ongoing in our laboratory.

This study has shown that noninvasive imaging of skin O_2sat could potentially be useful in monitoring the response of the microvasculature to shock and subsequent treatment. In particular, variations in cutaneous blood flow distribution and hemoglobin saturation as measured by HSI may offer new insights into the pathophysiology and treatment of shock. The skin is the body's largest and most accessible organ. Changes in the systemic

circulation are often manifested in the skin circulation. This has important implications not only for shock patients and in hypothermia, with the concomitant use as a portable field unit for the military, but also other disease conditions such as diabetes mellitus, where vascular degeneration can cause a significant reduction in the perfusion of the extremities. HSI is a novel and exciting means of measuring both the spatial and temporal variations in skin hemodynamics. Variations in cutaneous blood flow distribution and hemoglobin saturation, depicted by the HS images, may offer new insights into the pathophysiology and treatment of shock. The physiologic basis for and the clinical utility of these findings will be explored in further studies.

NOTE ADDED IN PROOF

At the time of revision, the authors had completed data collection and preliminary data analysis on a more statistically relevant group of animals ($n = 17$, nine shock, eight controls) using a hypovolemic shock model, albeit without the contusion in this study. There is a significant difference ($p << 0.05$) between shock and control animals, and a validation of the general findings of the study presented herein (J. Mansfield et al., manuscript in preparation).

ACKNOWLEDGMENTS

The opinions or assertions contained herein are the private views of the authors and are not to be construed as the official opinion of the Department of the Army, the Department of the Air Force, or the Department of Defense. The mention of specific products does not constitute an endorsement. This work was funded, in part, by the Medical Free Electron Laser program of the U.S. Department of Defense.

REFERENCES

1. Colarusso P, Kidder LH, Levin IW, Fraser JC, Arens JF, Lewis EN: Infrared spectroscopic imaging: from planetary to cellular systems. Appl Spectrosc 1998;52:106A–120A.
2. Treado PJ, Morris MD: Infrared and Raman spectroscopic imaging. Appl Spectrosc Rev 1994;29:1–38.
3. Paschalis EP, Verdelis K, Doty SB, Boskey AL, Mendelsohn R, Yamauchi M: Spectroscopic characterization of collagen cross-links in bone. J Bone Miner Res 2001;16:1821–1828.
4. Potter K, Kidder LH, Levin IW, Lewis EN, Spencer RG: Imaging of collagen and proteoglycan in cartilage sections using Fourier transform infrared spectral imaging. Arthritis Rheum 2001;44:846–855.
5. Zuzak KJ, Schaeberle MD, Gladwin MT, Cannon RO 3rd, Levin IW: Noninvasive determination of spatially resolved and time-resolved tissue perfusion in humans during nitric oxide inhibition and inhalation by use of a visible-reflectance hyperspectral imaging technique. Circulation 2001;104:2905–2910.
6. Mansfield JR, Sowa MG, Mantsch HH: Near infrared spectroscopic reflectance imaging: methods for functional imaging and in-vivo monitoring. Proc SPIE Int Soc Opt Eng 1999;3597:3297–3299.
7. Carlson KA, Jahr JS: A historical overview and update on pulse oximetry. Anesthesiol Rev 1993;20: 173–181.
8. Payette JR, Sowa MG, Germscheid SL, Stranc MF, Abdulrauf B, Mantsch HH: Noninvasive diagnostics: predicting flap viability with near-IR spectroscopy and imaging. Am Clin Lab 1999;18(3):4–6.
9. Sowa MG, Payette JR, Hewko MD, Mantsch HH: Visible–near infrared multispectral imaging of the rat dorsal skin flap. J Biomed Optics 1999;4:474–481.
10. Sowa MG, Leonardi L, Payette JR, Fish JS, Mantsch HH: Near infrared spectroscopic assessment of hemodynamic changes in the early post-burn period. Burns 2001;27:241–249.
11. Afromowitz MA, Callis JB, Heimbach DM, DeSoto LA, Norton MK: Multispectral imaging of burn wounds: a new clinical instrument for evaluating burn. IEEE Trans Biomed Eng 1988;35:842–850.
12. Chameides L, Haxinski MF, eds: Textbook of Pediatric Advanced Life Support. Dallas: American Heart Association, 1994.
13. Mansfield JR, Sowa MG, Scarth GB, Somorjai RL, Mantsch HH: The use of fuzzy C-means clustering in the analysis of spectroscopic imaging data. Anal Chem 1997;69:3370–3374.
14. Prall S. Available online at: http://omlc.ogi.edu/spectra/hemoglobin/index.html
15. Cancio LC, Brand D, Kerby J, Freeman JE, Hopmeier M, Mansfield JR: Visible hyperspectral imaging: monitoring the systemic effects of shock and resuscitation. Proc SPIE 2002;4614:159–168.
16. Wardell K, Braverman IM, Silverman DG, Nilsson GE: Spatial heterogeneity in normal skin perfusion recorded with laser Doppler imaging and flowmetry. Microvasc Res 1994;48:26–38.
17. Stauss HM, Stegmann JU, Persson PB, Habler HJ: Frequency response characteristics of sympathetic trans-

mission to skin vascular smooth muscles in rats. Am J Physiol 1999;277:R591–R600.
18. Bond RF, Bond CH, Johnson G 3rd: Intrinsic versus extrinsic regional vascular control during hemorrhagic hypotension and shock. Circ Shock 1986;18: 115–129.
19. Salerud EG, Tenland T, Nilsson GE, Oberg PA: Rhythmical variations in human skin blood flow. Int J Microcirc Clin Exp 1983;2:91–102.
20. Gniadecki R, Gniadecka M, Serup J: Examination of periodic fluctuations in cutaneous blood flow. In: Serup J, Jemec GB, eds. Handbook of Non-Invasive Methods and the Skin. Boca Raton, FL: CRC Press, 1995:411–420.
21. Roddie IC: Circulation to skin and adipose tissue. In: Shepherd JT, Abboud FM, eds. Handbook of Physiology, Sect 2: The Cardiovascular System, Vol. III: Peripheral Circulation and Organ Blood Flow, Part I. Bethesda, MD: American Physiological Society, 1983: 285–317.
22. Sakai H, Hara H, Tsai AG, Tsuchida E, Johnson PC, Intaglietta M: Changes in resistance vessels during hemorrhagic shock and resuscitation in conscious hamster model. Am J Physiol 1999;276(2 Pt 2):H563–H571.
23. Kerger H, Saltzman DJ, Menger MD, Messmer K, Intaglietta M: Systemic and subcutaneous microvascular pO_2 dissociation during 4-h hemorrhagic shock in conscious hamsters. Am J Physiol 1996;270(3 Pt 2): H827–H836.
24. Kerger H, Tsai AG, Saltzman DJ, Winslow RM, Intaglietta M: Fluid resuscitation with O_2 vs. non-O_2 carriers after 2 h of hemorrhagic shock in conscious hamsters. Am J Physiol 1997;272(1 Pt 2):H525–H537.
25. Bowles JH, Antoniades JA, Baumback MM, Grossmann JM, Haas D, Palmadesso PJ, Stracka J: Real-time analysis of hyperspectral data sets using NRL's ORASIS algorithm. Proc SPIE 1997;3118:38–45.
26. American College of Foot and Ankle Surgeons: Diabetic Foot Disorders: A Quick Reference Guide. Booklandville, MD: Data Trace Publishing Co., 2000.

Address reprint requests to:
James R. Mansfield, M.Sc.
HyperMed, Inc.
89 Bailey Road
Watertown, MA 02472

E-mail: jim@jmansfield.com